Proceedings of the 2006 IEEE International Conference on Robotics and Automation
Orlando, Florida - May 2006

System Identification for the Berkeley Lower Extremity Exoskeleton (BLEEX)

Justin Ghan and H. Kazerooni
Department of Mechanical Engineering
University of California, Berkeley
Berkeley, CA 94720, USA
Email: exo@me.berkeley.edu

***Abstract*— The exoskeleton is an autonomous robotic device whose function is to increase the strength and endurance of a human pilot. In order to achieve an exoskeleton controller which reacts compliantly to external forces, an accurate model of the dynamics of the system is required. In this report, a series of system identification experiments are designed and carried out for the Berkeley Lower Extremity Exoskeleton. As well as determining the mass and inertia properties of the segments of the legs, various non-ideal elements such as friction, stiffness and damping forces are identified. The resulting dynamic model is found to be significantly more accurate than the original model predicted from the designs of the robot.**

I. Introduction

The Berkeley Lower Extremity Exoskeleton (BLEEX) is a robotic device to be worn by a human in order to augment the strength and endurance of the wearer. The first generation model, developed at U.C. Berkeley's Human Engineering and Robotics Laboratory, is shown in Fig. 1. The exoskeleton controller is designed to allow a human to move around naturally wearing the exoskeleton robot, and not feel significant forces from the device [1]. In order to achieve such compliancy, the model of the system dynamics needs to be very accurate [2].

The dynamics of the exoskeleton can be predicted theoretically using the simplified model of the robot leg as a three segment manipulator, with the mass and inertia properties of the robot links predicted from design models [3]. However, a large number of factors affecting the dynamics cannot be predicted from this approach. Many parts of the robot cannot be modelled accurately, for example, the dynamics of the hosing and wiring, and the internal dynamics of the actuators. Additionally, there are many unknown forces acting within the robot, caused by friction, stiffness and damping of various elements.

Therefore, the model of the robot must be obtained experimentally. This report discusses the identification of the dynamics of a leg of the robot which is not in contact with the ground. This is called the swing mode of the leg, as opposed to the stance mode when the foot is touching the ground. During walking, the motions of a leg while in swing mode are generally faster and larger than those while in stance mode. Therefore, it is more important to have compliancy in the swing mode. For this reason, the system identification was first performed only for swing mode. However, the system identification methods used for the swing mode dynamics could be adapted to be used for the stance mode dynamics.

Fig. 1. The Berkeley Lower Extremity Exoskeleton.

II. Exoskeleton Dynamics

A. Three-Segment Model

The exoskeleton comprises two robotic legs attached to a torso. For the purposes of this investigation, the two legs have three degrees of freedom: a hip joint, a knee joint and an ankle joint, each of which is actuated by a hydraulic piston commanded by the controller. The leg is constrained to move within the sagittal plane.

0-7803-9505-0/06/$20.00 ©2006 IEEE

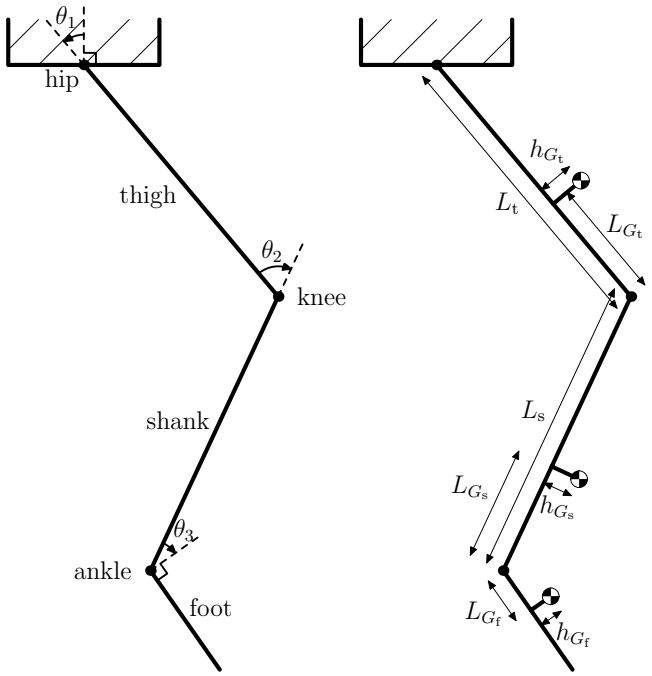

Fig. 2. Three segment model of the exoskeleton leg.

Each leg of the exoskeleton can be modelled as a two-dimensional three-segment manipulator, as described in [3]. A diagram of the simplified model is shown in Fig. 2. The length of the thigh link is L_t, and the length of the shank link is L_s. The position of the centre of gravity of the thigh is given by L_{G_t} and h_{G_t}, that of the shank by L_{G_s} and h_{G_s}, and that of the foot by L_{G_f} and h_{G_f}, as shown.

The joint angles θ_1, θ_2 and θ_3 are defined as shown in the diagram. If all joint angles are zero, then the thigh and shank are vertical and the foot is horizontal. The joint angle is positive if the angle of the lower link relative to the upper link is anti-clockwise.

At each joint, there will be a torque acting between the two links. The torque T_1 acts between the torso and the thigh, the torque T_2 acts between the thigh and the shank, and the torque T_3 acts between the shank and the foot. The sign convention is such that a positive torque T_i will cause a positive acceleration $\ddot{\theta}_i$.

The mass of the thigh, shank and foot links are m_t, m_s and m_f respectively. The moment of inertias of the links about their centres of gravity are I_t, I_s and I_f.

B. Ideal Equations of Motion

The derivation of the equations of motion for the simplified model of the exoskeleton leg is discussed in [3]. It is assumed that the only forces acting on the links are the joint torques, T_1, T_2 and T_3, and gravitational forces. Then expressions can be found for T_1, T_2 and T_3 in terms of the joint angles, $(\theta_1, \theta_2, \theta_3)$, the joint velocities, $(\dot{\theta}_1, \dot{\theta}_2, \dot{\theta}_3)$, the joint accelerations, $(\ddot{\theta}_1, \ddot{\theta}_2, \ddot{\theta}_3)$, and the constant geometry and mass parameters of the three links, $(L_\mathrm{t}, L_\mathrm{s}, L_{G_\mathrm{t}}, h_{G_\mathrm{t}}, L_{G_\mathrm{s}}, h_{G_\mathrm{s}}, L_{G_\mathrm{f}}, h_{G_\mathrm{f}}, m_\mathrm{t}, m_\mathrm{s}, m_\mathrm{f}, I_\mathrm{t}, I_\mathrm{s}, I_\mathrm{f})$.

The lengths of the thigh and shank links, L_t and L_s, may be determined by direct measurement of the distances between the centres of the joints, so these parameters are known.

The form of the equations in [3] are unsuitable for use in system identification, as it can be shown that the parameters appearing in those equations cannot be determined experimentally. The equations will be rewritten here in terms of the following nine new parameters.

$$X_3 = -m_\mathrm{f} h_{G_\mathrm{f}}, \tag{1}$$
$$Y_3 = m_\mathrm{f} L_{G_\mathrm{f}}, \tag{2}$$
$$X_2 = m_\mathrm{s}(L_\mathrm{s} - L_{G_\mathrm{s}}) + m_\mathrm{f} L_\mathrm{s}, \tag{3}$$
$$Y_2 = m_\mathrm{s} h_{G_\mathrm{s}}, \tag{4}$$
$$X_1 = m_\mathrm{t}(L_\mathrm{t} - L_{G_\mathrm{t}}) + m_\mathrm{s} L_\mathrm{t} + m_\mathrm{f} L_\mathrm{t}, \tag{5}$$
$$Y_1 = m_\mathrm{t} h_{G_\mathrm{t}}, \tag{6}$$
$$J_3 = I_\mathrm{f} + m_\mathrm{f}\left(h_{G_\mathrm{f}}^2 + L_{G_\mathrm{f}}^2\right), \tag{7}$$
$$J_2 = J_3 + I_\mathrm{s} + m_\mathrm{s}\left((L_\mathrm{s} - L_{G_\mathrm{s}})^2 + h_{G_\mathrm{s}}^2\right) + m_\mathrm{f} L_\mathrm{s}^2, \tag{8}$$
$$J_1 = J_2 + I_\mathrm{t} + m_\mathrm{t}\left((L_\mathrm{t} - L_{G_\mathrm{t}})^2 + h_{G_\mathrm{t}}^2\right) + m_\mathrm{s} L_\mathrm{t}^2 + m_\mathrm{f} L_\mathrm{t}^2. \tag{9}$$

Then the dynamic equations for the leg in swing mode can be rewritten in terms of these nine new parameters. The torque equation for the ankle joint is

$$\begin{aligned} T_3 = {} & \big[J_3 + L_\mathrm{s}(X_3\cos\theta_3 - Y_3\sin\theta_3) \\ & + L_\mathrm{t}(X_3\cos\theta_{23} - Y_3\sin\theta_{23})\big]\ddot{\theta}_1 \\ & + \big[J_3 + L_\mathrm{s}(X_3\cos\theta_3 - Y_3\sin\theta_3)\big]\ddot{\theta}_2 \\ & + \big[J_3\big]\ddot{\theta}_3 \\ & + L_\mathrm{t}(X_3\sin\theta_{23} + Y_3\cos\theta_{23})\,\dot{\theta}_1^2 \\ & + L_\mathrm{s}(X_3\sin\theta_3 + Y_3\cos\theta_3)\,\dot{\theta}_{12}^2 \\ & + g(X_3\sin\theta_{123} + Y_3\cos\theta_{123}). \end{aligned} \tag{10}$$

Note that θ_{12} denotes $\theta_1 + \theta_2$, θ_{23} denotes $\theta_2 + \theta_3$, and θ_{123} denotes $\theta_1 + \theta_2 + \theta_3$. Similarly, $\dot{\theta}_{12}$ denotes $\dot{\theta}_1 + \dot{\theta}_2$, and so on.

The torque equation for the knee joint is

$$\begin{aligned} T_2 = {} & \big[J_2 + 2L_\mathrm{s}(X_3\cos\theta_3 - Y_3\sin\theta_3) \\ & + L_\mathrm{t}(X_3\cos\theta_{23} - Y_3\sin\theta_{23}) \\ & + L_\mathrm{t}(X_2\cos\theta_2 - Y_2\sin\theta_2)\big]\ddot{\theta}_1 \\ & + \big[J_2 + 2L_\mathrm{s}(X_3\cos\theta_3 - Y_3\sin\theta_3)\big]\ddot{\theta}_2 \\ & + \big[J_3 + L_\mathrm{s}(X_3\cos\theta_3 - Y_3\sin\theta_3)\big]\ddot{\theta}_3 \\ & + L_\mathrm{t}(X_2\sin\theta_6 + Y_2\cos\theta_6)\,\dot{\theta}_1^2 \\ & + L_\mathrm{t}(X_3\sin\theta_{23} + Y_3\cos\theta_{23})\,\dot{\theta}_1^2 \\ & + L_\mathrm{s}(X_3\sin\theta_3 + Y_3\cos\theta_3)\left(\dot{\theta}_{12}^2 - \dot{\theta}_{123}^2\right) \\ & + g(X_2\sin\theta_{12} + Y_2\cos\theta_{12} \\ & + X_3\sin\theta_{123} + Y_3\cos\theta_{123}). \end{aligned} \tag{11}$$

Finally, the torque equation for the hip joint is

$$\begin{aligned}
T_1 = &\big[J_1 + 2L_s(X_3\cos\theta_3 - Y_3\sin\theta_3) \\
&\quad + 2L_t(X_3\cos\theta_{23} - Y_3\sin\theta_{23}) \\
&\quad + 2L_t(X_2\cos\theta_2 - Y_2\sin\theta_2)\big]\ddot{\theta}_1 \\
&+ \big[J_2 + 2L_s(X_3\cos\theta_3 - Y_3\sin\theta_3) \\
&\quad + L_t(X_3\cos\theta_{23} - Y_3\sin\theta_{23}) \\
&\quad + L_t(X_2\cos\theta_2 - Y_2\sin\theta_2)\big]\ddot{\theta}_2 \\
&+ \big[J_3 + L_s(X_3\cos\theta_3 - Y_3\sin\theta_3) \\
&\quad + L_t(X_3\cos\theta_{23} - Y_3\sin\theta_{23})\big]\ddot{\theta}_3 \\
&+ L_t(X_2\sin\theta_6 + Y_2\cos\theta_6)\left(\dot{\theta}_1^2 - \dot{\theta}_{12}^2\right) \\
&+ L_t(X_3\sin\theta_{23} + Y_3\cos\theta_{23})\left(\dot{\theta}_1^2 - \dot{\theta}_{123}^2\right) \\
&+ L_s(X_3\sin\theta_3 + Y_3\cos\theta_3)\left(\dot{\theta}_{12}^2 - \dot{\theta}_{123}^2\right) \\
&+ g(X_1\sin\theta_1 + Y_1\cos\theta_1 \\
&\quad + X_2\sin\theta_{12} + Y_2\cos\theta_{12} \\
&\quad + X_3\sin\theta_{123} + Y_3\cos\theta_{123}). \qquad (12)
\end{aligned}$$

It can be shown that these nine parameters, X_3, Y_3, X_2, Y_2, X_1, Y_1, J_3, J_2, and J_1, are independent and can therefore be identified via experiment. They are a minimal set of parameters which fully describe the dynamics of the system.

Note that these equations apply to the case where the torso is stationary, which is the case for all experiments described in this report. However, if the dynamic equations are re-derived for the case when the torso is in motion, they can also be expressed in terms of only this reduced set of nine parameters. Therefore, it is still sufficient to identify only these parameters.

C. Friction, Stiffness and Damping

Let A_i denote the torque exerted on the joint by the hydraulic actuator. An accurate estimate of this torque can be obtained from the force sensor measurement, and the joint angle encoder measurement. (The joint angle is required to calculate the moment arm of the actuator force about the joint.)

There are several other torques acting on the joint. We divide these into three components: a stiffness torque, a damping and kinetic friction torque, and a static friction torque. The stiffness torque, which we denote by B_i, is expected to be a function only of the joint angle, that is, $B_i = b_i(\theta_i)$. The damping and kinetic friction torque, which we denote by C_i, is expected to be a function only of the joint angular velocity, that is, $C_i = c_i(\dot{\theta}_i)$. This torque C_i is zero when $\dot{\theta}_i$ is zero. Finally, the static friction torque is denoted by D_i.

The total torque exerted on the joint is then given by the equation

$$T_i = A_i + B_i + C_i + D_i. \qquad (13)$$

D. Parameters for Identification

In order to have an accurate model of the relationship between the actuator torques and the motion of the exoskeleton, all terms in the equations above must be characterised.

The following parameters are known:

- the link lengths, L_t, L_s, and
- the gravitational constant, g.

The terms which need to be identified are:

- the mass moment parameters, X_3, Y_3, X_2, Y_2, X_1, Y_1,
- the inertial parameters, J_3, J_2, J_1,
- the stiffness torques, B_3, B_2, B_1 and
- the damping and kinetic friction torques, C_3, C_2, C_1.

The static friction torques, D_3, D_2, D_1, will not be characterised, for reasons described later.

III. Parameter Identification

A. Least Squares Estimation

Least squares estimation can be used to identify parameters in systems, when we have a linear relationship between the unknown parameters with coefficients which are known functions of measurable quantities [4]–[8]. For example, suppose we have a system governed by the equation

$$y(t) = [\boldsymbol{h}(t)]^T\boldsymbol{x}. \qquad (14)$$

Here, $\boldsymbol{x}$ is a vector of n constant unknown parameters, $y(t)$ is the output of the system at time t, and the n coefficients in the vector $\boldsymbol{h}(t)$ are time-varying and depend upon the state of the system. However, we can determine $\boldsymbol{h}(t)$ from measurable quantities.

To estimate the unknown parameters, we take measurements $y(t_i)$ of the system output at m different times or configurations. At each of these times or configurations, we calculate the the coefficients vector, $\boldsymbol{h}(t_i)$. Additionally, some noise $v(t_i)$ is introduced into each measurement, so that $y(t_i) = [\boldsymbol{h}(t_i)]^T\boldsymbol{x} + v(t_i)$. Then, we can write these m equations in matrix form,

$$\boldsymbol{y} = H\boldsymbol{x} + \boldsymbol{v}. \qquad (15)$$

where

$$\boldsymbol{y} = \begin{bmatrix} y(t_1) \\ y(t_2) \\ \vdots \\ y(t_m) \end{bmatrix}, \quad \boldsymbol{v} = \begin{bmatrix} v(t_1) \\ v(t_2) \\ \vdots \\ v(t_m) \end{bmatrix},$$

$$H = \begin{bmatrix} [\boldsymbol{h}(t_1)]^T \\ [\boldsymbol{h}(t_2)]^T \\ \vdots \\ [\boldsymbol{h}(t_m)]^T \end{bmatrix}. \qquad (16)$$

Then we can find a least squares estimate $\hat{\boldsymbol{x}}$ using the equation

$$\hat{\boldsymbol{x}} = \left(H^TH\right)^{-1}H^T\boldsymbol{y}. \qquad (17)$$

B. Experimental Procedure

In this section, the experimental procedures followed in collecting data for the parameter identification process are outlined.

1) Static Experiments: The static experiments are those in which the joint torques are measured when the exoskeleton is in a static configuration, so all joint velocities and accelerations are zero. For each experiment, the exoskeleton is placed on a jig so that the torso is held in the air at a fixed position and in vertical orientation. A sequence of configurations is programmed into the exoskeleton controller. Each configuration consists of a list of six joint angles, $(\theta_{1_\mathrm{L}}, \theta_{2_\mathrm{L}}, \theta_{3_\mathrm{L}}, \theta_{1_\mathrm{R}}, \theta_{2_\mathrm{R}}, \theta_{3_\mathrm{R}})$. When the controller is activated, the six actuators are each commanded to move the joint to the desired angle, θ_d.

The voltage sent to the actuators, u, is determined by a simple proportional controller, $u = -K_P(\theta - \theta_\mathrm{d})$, where θ is the joint angle measured by the encoder. After the joints have stopped moving, the data from each of the force sensors are collected. The joint angles measured by the encoders are also recorded. From these values, the torque exerted by the actuator at each of the six joints is calculated and recorded.

2) Dynamic Experiments: In the dynamic experiments, the joint torques are measured when the exoskeleton is in motion. A trajectory of the robot configuration is programmed into the exoskeleton controller. The trajectory consists of a list of six joint angle trajectories, $(\theta_{1_\mathrm{L}}(t), \theta_{2_\mathrm{L}}(t), \theta_{3_\mathrm{L}}(t), \theta_{1_\mathrm{R}}(t), \theta_{2_\mathrm{R}}(t), \theta_{3_\mathrm{R}}(t))$. When the controller is activated, the six actuators are each commanded to track the desired trajectory, $\theta_\mathrm{d}(t)$. As in the static experiments, a simple proportional controller is used to determine the voltage sent to the actuators.

The joint encoder and force sensor readings are recorded at a rate of $f_\mathrm{s} \approx 50\,\mathrm{Hz}$. At each sample point, the torque exerted by the actuator at each of the six joints is calculated from the joint encoder and force sensor readings and recorded.

After the experiment, the joint velocities and accelerations at each of the sample points (excepting the first and last) are estimated by finite difference approximations.

C. Static Friction Torques

When a robot leg is moved to a static configuration, $(\theta_1, \theta_2, \theta_3)$, the actuator torque for each joint depends on the direction from which the joint angle was reached. This phenomenon can be observed in the plot shown in Fig. 3. The hip and knee angles were held constant throughout this experiment. The ankle was moved cyclically through the angles $\{-15°, 0°, 15°, 0°\}$. On the actuator torque plot, the circles represent the torques A_3^+ where the angle position, $0°$, was approached from the negative, and the crosses represent the torques A_3^- where the angle position was approached from the positive. It can be seen that the torques A_3^+ are consistently greater than the torques A_3^-.

The discrepancy between A_i^+ and A_i^- is due to the static friction torque, D_i. When the joint is moving with positive velocity (θ_i increasing), there is a negative kinetic friction torque to oppose the motion. When the joint comes to rest, there remains a negative static friction torque. If the joint comes to rest from the other direction, the static friction torque will be positive.

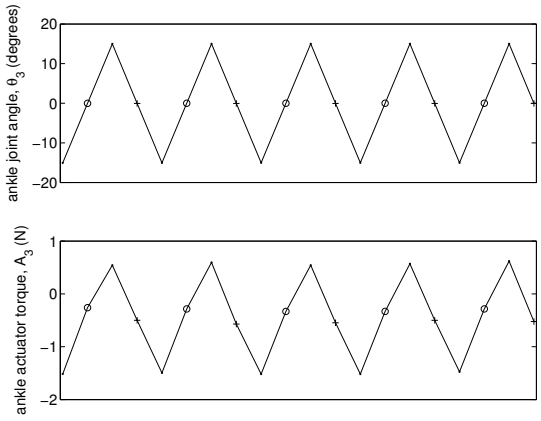

Fig. 3. Effect of the static friction torque in the ankle.

When the robot is walking, no joint will be completely static. Therefore, the controller does not need to be able to estimate the static friction torque, so there is no reason to characterise it. However, in order to obtain accurate results in the estimation of the other parameters, it is desirable to reduce the effects of the static friction torques. This can be achieved by taking each static torque measurement twice, first approaching the the joint angle θ_i from the negative direction, then approaching it from the positive direction. The two torques obtained, A_i^+ and A_i^-, are then averaged to obtain an estimate of what the actuator torque would be if there were no static friction torque.

D. Stiffness Torques

When the robot is static ($\dot\theta_1 = \dot\theta_2 = \dot\theta_3 = 0$ and $\ddot\theta_1 = \ddot\theta_2 = \ddot\theta_3 = 0$), the ankle joint torque given by (10) becomes

$$T_3 = g(X_3 \sin\theta_{123} + Y_3 \cos\theta_{123}). \tag{18}$$

Also, under static conditions, the damping and kinetic friction torque, C_3, is zero. We eliminate the static friction torque, D_3, by averaging two measurements as discussed in the previous section. Therefore, from (13), when the robot is static, the measured torque is

$$A_3 = g(X_3 \sin\theta_{123} + Y_3 \cos\theta_{123}) - B_3. \tag{19}$$

To identify the ankle stiffness torque, B_3, the robot was controlled to move to a series of positions such that θ_{123} was the same at each of the positions, while θ_1, θ_2 and θ_3 were all varied. Then the term $(X_3 \sin\theta_{123} + Y_3 \cos\theta_{123})$ is constant for the set of positions, so the measured torque is

$$A_3 = -B_3 + g(X_3 \sin\theta_{123} + Y_3 \cos\theta_{123}), \tag{20}$$

where $g(X_3 \sin\theta_{123} + Y_3 \cos\theta_{123})$ is a constant.

The measured torque, A_3, was plotted against the ankle joint angle, θ_3. The experiment was repeated for several different values of θ_{123}. The different data sets were found to have the same shape, as shown in Fig. 4, supporting the assumption that B_3 is a function only of θ_3, so we can write $B_3 = b_3(\theta_3)$.

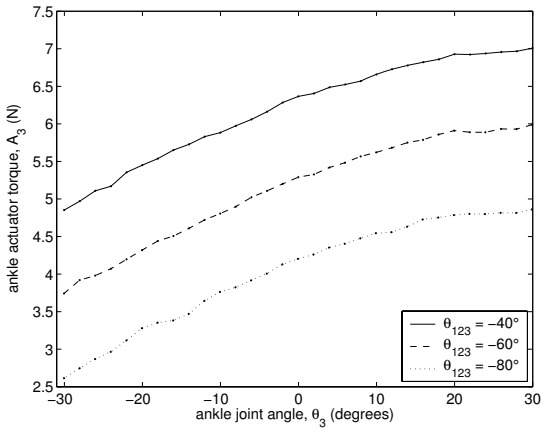

Fig. 4. Effects of the stiffness torque in the ankle for various values of θ_{123}.

It was found that a quadratic function, $b_{23}\theta_3^2 + b_{13}\theta_3 + c$, fit the resulting plots very closely. The parameters b_{23} and b_{13} were determined using a least squares fit. Then our characterisation of the stiffness function is

$$b_3(\theta_3) = b_{23}\theta_3^2 + b_{13}\theta_3 + b_{03}. \tag{21}$$

However, the parameter b_{03} could not be determined from the previous data alone, since the constants $g(X_3 \sin\theta_{123} + Y_3 \cos\theta_{123})$ for each value of θ_{123} were unknown.

In order to find the parameter b_{03}, the robot was controlled to two positions, $(\theta_1, \theta_2, \theta_3)$ and $(\theta_1', \theta_2', \theta_3')$, such that $\theta_1' + \theta_2' = \theta_1 + \theta_2 + 180°$ and $\theta_3' = \theta_3$. The measured torques are

$$A_3 = -b_3(\theta_3) + g(X_3 \sin\theta_{123} + Y_3 \cos\theta_{123}), \tag{22}$$

$$A_3' = -b_3(\theta_3') + g(X_3 \sin\theta_{123}' + Y_3 \cos\theta_{123}'). \tag{23}$$

Since $\theta_{123}' = \theta_{123} + 180°$, it can be shown that

$$b_3(\theta_3) = -\frac{A_3 + A_3'}{2}. \tag{24}$$

Therefore, from these two torque measurements, and using our previously determined values of b_{23} and b_{13}, we obtain an estimate of b_{03},

$$b_{03} = -\frac{A_3 + A_3'}{2} - b_{23}\theta_3^2 - b_{13}\theta_3. \tag{25}$$

By taking a large number of pairs of torque measurements of this kind, and averaging the resulting values of b_{03}, we can determine b_{03}.

The procedure for identifying the stiffness torque in the knee joint is very similar. As for the ankle, we find that the knee actuator torques are dependent only on the knee joint angle, so $B_2 = b_2(\theta_2)$. Our characterisation of the stiffness function is

$$b_2(\theta_2) = b_{22}\theta_2^2 + b_{12}\theta_2 + b_{02}, \tag{26}$$

and the three parameters b_{22}, b_{12} and b_{02} are identified.

Finding the stiffness torque in the hip joints is much more difficult than finding the stiffness torques in the knee and ankle joints. In principle, a method similar to those used for the knee and ankle joints could be used, but this would require experiments with the exoskeleton torso mounted in many different orientations, so that the hip joint angle would change while the gravitational torque on the hip remained constant.

There is no reason that the magnitude of the stiffness torque in the hip joints should be greater (or smaller) than that in the knee and ankle joints. However, the total torque in the hip joint is in general significantly greater in magnitude than that in the knee and ankle joints. Therefore, the relative impact of the stiffness torque on the total torque is much less significant in the hip joint than in the other joints.

For these reasons, the stiffness torque in the hip joints was not identified. The best estimate without experimental data is $B_1 = 0$.

E. Mass Moment Parameters

Equation (19) is the ankle torque equation under static conditions. Substituting in (21) for the ankle stiffness torque and rearranging yields

$$\begin{aligned} &g(X_3 \sin\theta_{123} + Y_3 \cos\theta_{123}) \\ &\quad = A_3 + (b_{23}\theta_3^2 + b_{13}\theta_3 + b_{03}). \end{aligned} \tag{27}$$

The robot is controlled to move to a series of 100 static configurations, and the joint angles and the ankle joint torque are measured at each one. Then, for each configuration, the right hand side of (27), $A_3 + b_{23}\theta_3^2 + b_{13}\theta_3 + b_{03}$, is known, because the parameters b_{23}, b_{13} and b_{03} have been identified. Additionally, on the left hand side, the gravitational constant g is known, and the values $\sin\theta_{123}$ and $\cos\theta_{123}$ can be calculated. Therefore, we can use a least squares fitting to estimate X_3 and Y_3 from these measurements.

We can find the knee and hip mass moment parameters in an identical manner.

F. Inertia Parameters

1) Foot Inertia Parameter: When the ankle and hip joints are stationary ($\ddot{\theta}_1 = \ddot{\theta}_3 = 0$, $\dot{\theta}_1 = \dot{\theta}_3 = 0$), then the torque equation for the ankle joint is

$$\begin{aligned} T_3 = &\left[J_3 + L_s(X_3 \cos\theta_3 - Y_3 \sin\theta_3)\right]\ddot{\theta}_2 \\ &+ L_s(X_3 \sin\theta_3 + Y_3 \cos\theta_3)\,\dot{\theta}_2^2 \\ &+ g(X_3 \sin\theta_{123} + Y_3 \cos\theta_{123}). \end{aligned} \tag{28}$$

Neglecting the friction torque, D_3, which is small compared to the total dynamic ankle torque, the left hand side of this equation is equal to $A_3 + B_3 + C_3$. We know $C_3 = 0$, since $\dot{\theta}_3 = 0$. Therefore, we have

$$\begin{aligned} &\left[J_3 + L_s(X_3 \cos\theta_3 - Y_3 \sin\theta_3)\right]\ddot{\theta}_2 \\ &\quad = A_3 + B_3 - L_s(X_3 \sin\theta_3 + Y_3 \cos\theta_3)\,\dot{\theta}_2^2 \\ &\qquad - g(X_3 \sin\theta_{123} + Y_3 \cos\theta_{123}), \end{aligned} \tag{29}$$

where the right hand side of the equation is known, since X_3 and Y_3 have been identified. The only unknown is the foot inertia parameter, J_3. The coefficient of $\ddot{\theta}_2$ is a constant, since the ankle joint angle θ_3 is fixed.

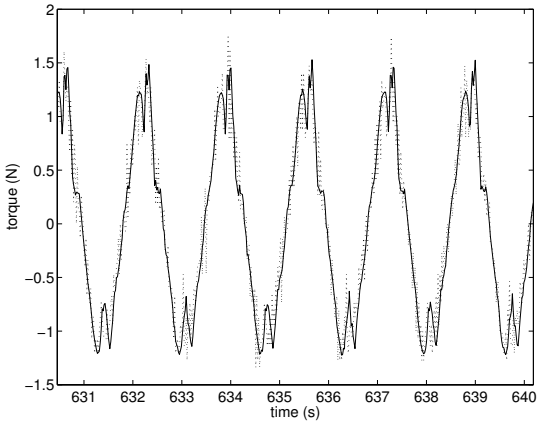

Fig. 5. The inertial component of the ankle joint torque.

To identify the parameter J_3, the hip and ankle joints were controlled to fixed positions, while the knee joint was controlled to track a sinusoidal input of fixed frequency. The joint angles and ankle joint torque were recorded. This was repeated for five different frequencies (0.2 Hz, 0.4 Hz, 0.6 Hz, 0.8 Hz, 1.0 Hz).

A least squares fitting was then used to estimate the value of $[J_3 + L_s(X_3 \cos\theta_3 - Y_3 \sin\theta_3)]$ from this data. Finally, the known values of L_s, X_3 and Y_3, along with the constant value of θ_3 for the experiments, were used to obtain an estimate of the foot inertia parameter, J_3.

A plot of the fit for one of the experiments is shown in Fig. 5. The solid line shows the right hand side of (29) calculated from the torque and joint angle measurements. The dotted line shows the left hand side of (29) calculated using the the value of J_3 obtained from the least squares fitting. The plots matched well for all of the experiments, verifying the form of the equation.

2) Shank Inertia Parameter: When the ankle and knee joints are stationary ($\ddot{\theta}_2 = \ddot{\theta}_3 = 0$, $\dot{\theta}_2 = \dot{\theta}_3 = 0$), neglecting the friction torque, D_2, we have

$$\begin{aligned}
&\big[J_2 + 2L_s(X_3 \cos\theta_3 - Y_3 \sin\theta_3) \\
&\quad + L_t(X_3 \cos\theta_{23} - Y_3 \sin\theta_{23}) \\
&\quad + L_t(X_2 \cos\theta_2 - Y_2 \sin\theta_2)\big]\ddot{\theta}_1 \\
&= A_2 + B_2 - L_t(X_2 \sin\theta_2 + Y_2 \cos\theta_2)\,\dot{\theta}_1^2 \\
&\quad - L_t(X_3 \sin\theta_{23} + Y_3 \cos\theta_{23})\,\dot{\theta}_1^2 \\
&\quad - g(X_2 \sin\theta_{12} + Y_2 \cos\theta_{12} \\
&\quad + X_3 \sin\theta_{123} + Y_3 \cos\theta_{123}),
\end{aligned} \tag{30}$$

where the right hand side of the equation is known, since X_3, Y_3, X_2 and Y_2 have been identified. The only unknown is the shank inertia parameter, J_2. The coefficient of $\ddot{\theta}_1$ is a constant, since the knee and ankle joint angles θ_2 and θ_3 are fixed.

To identify the parameter J_2, the knee and ankle joints were controlled to fixed positions, while the hip joint was controlled to track a sinusoidal input of fixed frequency. The joint angles and ankle joint torque were recorded. This was repeated for five different frequencies (0.2 Hz, 0.4 Hz, 0.6 Hz, 0.8 Hz, 1.0 Hz).

A least squares fitting was then used to estimate the value of

$$\begin{aligned}
&\big[J_2 + 2L_s(X_3 \cos\theta_3 - Y_3 \sin\theta_3) \\
&\quad + L_t(X_3 \cos\theta_{23} - Y_3 \sin\theta_{23}) \\
&\quad + L_t(X_2 \cos\theta_2 - Y_2 \sin\theta_2)\big]
\end{aligned}$$

from this data. Finally, the known values of L_s, L_t, X_3, Y_3, X_2 and Y_2, along with the constant values of θ_2 and θ_3 for the experiments, were used to obtain an estimate of the shank inertia parameter, J_2.

The results were verified by plotting the right hand side of (30) calculated from the torque and joint angle measurements against the left hand side calculated using the the value of J_2 obtained. Again, the plots matched well for all of the experiments, verifying the form of the equation.

3) Thigh Inertia Parameter: When the ankle and knee joints are stationary ($\ddot{\theta}_2 = \ddot{\theta}_3 = 0$, $\dot{\theta}_2 = \dot{\theta}_3 = 0$), neglecting both the friction torque, D_1, and the damping and kinetic friction torque C_1, we have

$$\begin{aligned}
&\big[J_1 + 2L_s(X_3 \cos\theta_3 - Y_3 \sin\theta_3) \\
&\quad + 2L_t(X_3 \cos\theta_{23} - Y_3 \sin\theta_{23}) \\
&\quad + 2L_t(X_2 \cos\theta_2 - Y_2 \sin\theta_2)\big]\ddot{\theta}_1 \\
&= A_1 - g(X_1 \sin\theta_1 + Y_1 \cos\theta_1 \\
&\quad + X_2 \sin\theta_{12} + Y_2 \cos\theta_{12} \\
&\quad + X_3 \sin\theta_{123} + Y_3 \cos\theta_{123}),
\end{aligned} \tag{31}$$

where the right hand side of the equation is known, since X_3, Y_3, X_2, Y_2, X_1 and Y_1 have been identified. The only unknown is the thigh inertia parameter, J_1. The coefficient of $\ddot{\theta}_1$ is a constant, since the joint angles θ_2 and θ_3 are fixed.

To identify the parameter J_1, the ankle and knee joints were controlled to fixed positions, while the hip joint was controlled to track a sinusoidal input of fixed frequency. The joint angles and hip joint torque were recorded. This was repeated for five different frequencies (0.2 Hz, 0.4 Hz, 0.6 Hz, 0.8 Hz, 1.0 Hz).

A least squares fitting was then used to estimate the value of

$$\begin{aligned}
&\big[J_1 + 2L_s(X_3 \cos\theta_3 - Y_3 \sin\theta_3) \\
&\quad + 2L_t(X_3 \cos\theta_{23} - Y_3 \sin\theta_{23}) \\
&\quad + 2L_t(X_2 \cos\theta_2 - Y_2 \sin\theta_2)\big]
\end{aligned}$$

from this data. Finally, the known values of L_s, L_t, X_3, Y_3, X_2 and Y_2, along with the constant values of θ_2 and θ_3 for the experiments, were used to obtain an estimate of the thigh inertia parameter, J_1.

The results were verified by plotting the right hand side of (31) calculated from the torque and joint angle measurements against the left hand side calculated using the the value of J_2 obtained. Again, the plots matched well for all of the experiments, verifying the form of the equation.

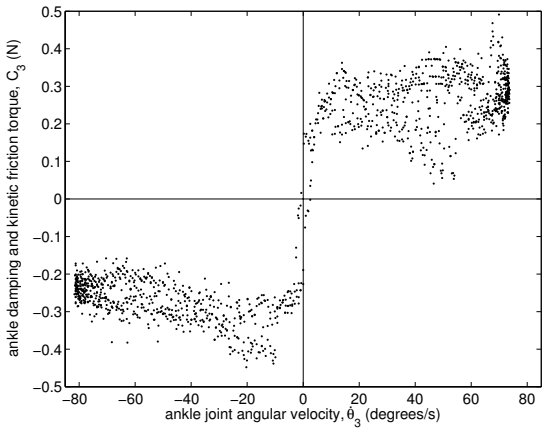

Fig. 6. The ankle damping and kinetic friction torque, C_3.

G. Damping and Kinetic Friction Torques

When the hip and knee joints are stationary ($\ddot{\theta}_1 = \ddot{\theta}_2 = 0$, $\dot{\theta}_1 = \dot{\theta}_2 = 0$), then the torque equation for the ankle joint is

$$T_3 = \big[J_3\big]\ddot{\theta}_3 + g(X_3 \sin\theta_{123} + Y_3 \cos\theta_{123}). \tag{32}$$

If the ankle joint is in motion, then the static friction torque, D_3, is zero. Then the left hand side of this equation is equal to $A_3 + B_3 + C_3$. The actuator torque A_3 is measured, and the stiffness torque B_3 can be calculated from the joint angle using the stiffness function $b_3(\theta_3)$ found in Section III-D. Therefore, the right hand side of the equation

$$C_3 = \big[J_3\big]\ddot{\theta}_3 + g(X_3 \sin\theta_{123} + Y_3 \cos\theta_{123}) - A_3 - B_3, \tag{33}$$

is known. The damping and kinetic friction torque, C_3, is expected to be a function of the joint angular velocity, $C_3 = c_3(\dot{\theta}_3)$.

To find the damping and kinetic friction function, $c_3(\dot{\theta}_3)$, the hip and knee joints were controlled to fixed positions, while the ankle joint was controlled to track a sinusoidal input of fixed frequency. The joint angles and ankle joint torque were recorded. This was repeated for five different frequencies ($0.2\,\text{Hz}$, $0.4\,\text{Hz}$, $0.6\,\text{Hz}$, $0.8\,\text{Hz}$, $1.0\,\text{Hz}$).

The damping and kinetic friction torque, C_3, was calculated from (33). A plot of C_3 against the joint angular velocity, $\dot{\theta}_3$, for one of the experiments is shown in Fig. 6.

It can be seen that the torque C_3 is approximately proportional to $\operatorname{sgn}\dot{\theta}_3$. The same result was found in all experiments. This shows that there is very little damping torque, which would be approximately proportional to $\dot{\theta}_3$. There is only a kinetic friction torque, of the form

$$c_3(\dot{\theta}_3) = c_{03} \operatorname{sgn}\dot{\theta}_3. \tag{34}$$

The constant of proportionality, c_{03}, was found using a least squares fitting to the data from several different frequencies. (Data points with $\dot{\theta}_3$ close to 0 were discarded, due to the discontinuity in $\operatorname{sgn}\dot{\theta}_3$.)

The procedure for identifying the damping and kinetic friction torque in the knee joint is very similar. As for the ankle, we find that there is very little damping torque, but only a kinetic friction torque of the form

$$c_2(\dot{\theta}_2) = c_{02} \operatorname{sgn}\dot{\theta}_2, \tag{35}$$

and the constant of proportionality, c_{02}, is identified.

However, the damping and kinetic friction torque in the hip joint was unable to be identified using the same method as was used to determine those in the ankle and knee joints, due to the larger errors in the identification of X_1, Y_1 and J_1.

It would be expected that the kinetic friction torques in the hip are the same order of magnitude as those in the knee and ankle joints. Since the total torque in the hip joint is in general significantly greater in magnitude than that in the knee and ankle joints, the relative impact of the kinetic friction torque on the total torque is much less significant in the hip joint than in the other joints.

For these reasons, the damping and kinetic friction torque in the hip joints was not identified. The best estimate without experimental data is $C_1 = 0$.

IV. Analysis of Results

A. Summary of Numerical Results

The numerical results of the identification experiments are presented in Tables I–IV. As discussed, the stiffness torques and the damping and kinetic friction torques in the hip joints were not identified. The best estimate of these torques without experimental data are $B_1 = 0$ and $C_1 = 0$.

The mass moment parameters and inertia parameters can be compared to the values calculated by SolidWorks from the design models of the parts. The values are the same for the left and right legs, since the designs are identical. These are shown in Table V.

B. Comparison of Models

In order to evaluate the accuracy of the system model obtained from the system identification results, the exoskeleton was controlled to move each of its joints in a sinusoidal trajectory. The six actuator torques, A_i, were both measured via

TABLE I
STIFFNESS TORQUES

Left leg
$B_3 = (0.3129\,\text{N·m/rad}^2)\,\theta_3^2 + (0.1557\,\text{N·m/rad})\,\theta_3 + (-0.5829\,\text{N·m})$
$B_2 = (0.6263\,\text{N·m/rad}^2)\,\theta_2^2 + (1.9334\,\text{N·m/rad})\,\theta_2 + (0.5\,\text{N·m})$
Right leg
$B_3 = (-1.5341\,\text{N·m/rad}^2)\,\theta_3^2 + (2.1484\,\text{N·m/rad})\,\theta_3 + (4.5771\,\text{N·m})$
$B_2 = (1.2573\,\text{N·m/rad}^2)\,\theta_2^2 + (2.2442\,\text{N·m/rad})\,\theta_2 + (-1.0\,\text{N·m})$

TABLE II
MASS MOMENT PARAMETERS

Left leg	Right leg
$X_3 = 0.2552\,\text{kg·m}$	$X_3 = 0.2554\,\text{kg·m}$
$Y_3 = 0.1313\,\text{kg·m}$	$Y_3 = 0.1279\,\text{kg·m}$
$X_2 = 1.9628\,\text{kg·m}$	$X_2 = 1.9532\,\text{kg·m}$
$Y_2 = 0.0031\,\text{kg·m}$	$Y_2 = -0.0386\,\text{kg·m}$
$X_1 = 3.9819\,\text{kg·m}$	$X_1 = 4.0474\,\text{kg·m}$
$Y_1 = -0.4083\,\text{kg·m}$	$Y_1 = -0.4990\,\text{kg·m}$

TABLE III

INERTIA PARAMETERS

Left leg	Right leg
$J_3 = 0.04528\,\mathrm{kg{\cdot}m^2}$	$J_3 = 0.05243\,\mathrm{kg{\cdot}m^2}$
$J_2 = 0.7833\,\mathrm{kg{\cdot}m^2}$	$J_2 = 0.7897\,\mathrm{kg{\cdot}m^2}$
$J_1 = 2.380\,\mathrm{kg{\cdot}m^2}$	$J_1 = 2.598\,\mathrm{kg{\cdot}m^2}$

TABLE IV

KINETIC FRICTION TORQUES

Left leg	Right leg
$C_3 = -(0.2646\,\mathrm{N{\cdot}m})\,\mathrm{sgn}\,\dot{\theta}_3$	$C_3 = -(0.3370\,\mathrm{N{\cdot}m})\,\mathrm{sgn}\,\dot{\theta}_3$
$C_2 = -(0.5291\,\mathrm{N{\cdot}m})\,\mathrm{sgn}\,\dot{\theta}_2$	$C_2 = -(0.4081\,\mathrm{N{\cdot}m})\,\mathrm{sgn}\,\dot{\theta}_2$

TABLE V

SOLIDWORKS PARAMETERS

$X_3 = 0.2793\,\mathrm{kg{\cdot}m}$	$X_2 = 2.055\,\mathrm{kg{\cdot}m}$	$X_1 = 3.783\,\mathrm{kg{\cdot}m}$
$Y_3 = 0.1546\,\mathrm{kg{\cdot}m}$	$Y_2 = 0.05778\,\mathrm{kg{\cdot}m}$	$Y_1 = -0.1601\,\mathrm{kg{\cdot}m}$
$J_3 = 0.05628\,\mathrm{kg{\cdot}m^2}$	$J_2 = 0.8939\,\mathrm{kg{\cdot}m^2}$	$J_1 = 2.497\,\mathrm{kg{\cdot}m^2}$

the force sensors, and estimated from the identified parameters and functions identified experimentally.

The estimates of the actuator torques calculated from the system identification results were compared to the actual measured actuator torques. One set of results is shown in the dark black lines of Fig. 7. It can be seen that the calculated actuator torques closely match the measured actuator torques. Therefore, the results of the system identification provide a good model of the dynamics.

The light grey lines in Fig. 7 show the estimates of the actuator torques calculated from the model based on the SolidWorks designs of the exoskeleton. It can be seen that, in general, this model is significantly less accurate than the results using the system identification based model.

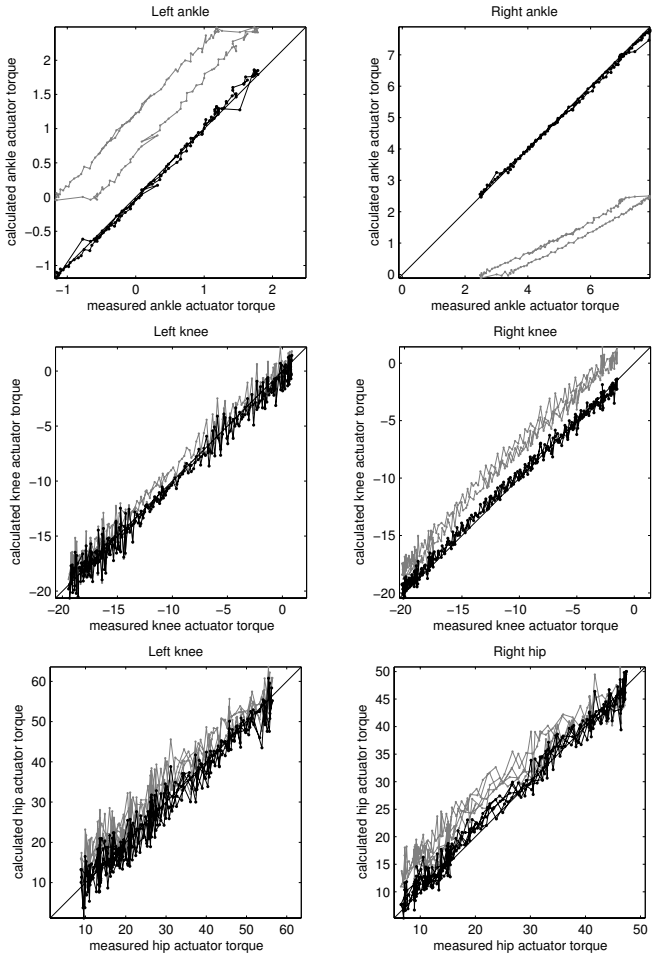

Fig. 7. Comparison of calculated actuator torques to measured actuator torques in a dynamic experiment.

V. CONCLUSIONS

A series of system identification experiments were designed and carried out for the lower extremity exoskeleton robot. The results of the identification process produced an accurate model of the dynamics of the exoskeleton legs. This model was compared to the simplistic model predicted from the robot designs, and was found to be much more accurate.

REFERENCES

[1] H. Kazerooni, J. L. Racine, L. Huang, and R. Steger, "On the control of the Berkeley Lower Extremity Exoskeleton (BLEEX)," in *IEEE Int. Conf. Robotics and Automation*, Barcelona, Spain, Apr. 2005.

[2] R. Steger, S. H. Kim, and H. Kazerooni, "Control scheme and networked control architecture for the Berkeley Lower Extremity Exoskeleton (BLEEX)," in *IEEE Int. Conf. Robotics and Automation*, Orlando, FL, May 2006, in press.

[3] J. L. Racine, "Control of a lower extremity exoskeleton for human performance amplification," Ph.D. dissertation, University of California, Berkeley, 2003.

[4] T. C. Hsia, *System identification*. Lexington Books, 1977.

[5] D. D. Joshi, *Linear estimation and design of experiments*. John Wiley & Sons, 1987.

[6] T. Kariya and H. Kurata, *Generalized least squares*. John Wiley & Sons, 2004.

[7] C. R. Rao and H. Toutenberg, *Linear models: least squares and alternatives*, 2nd ed. Springer-Verlag, 1999.

[8] H. W. Sorenson, *Parameter estimation*, ser. Control and systems theory. Marcel Dekker, 1980, vol. 9.